Hydration Structure of the Quaternary Ammonium Cations

ARTICLE *in* THE JOURNAL OF PHYSICAL CHEMISTRY B · OCTOBER 2010

Impact Factor: 3.3 · DOI: 10.1021/jp106282w · Source: PubMed

4 AUTHORS, INCLUDING:

Leonardo Guidoni
Università degli Studi dell'Aquila
90 PUBLICATIONS **1,435** CITATIONS

SEE PROFILE

Hydration Structure of the Quaternary Ammonium Cations

Wojtek Iwo Babiaczyk,*,†,‡ Sara Bonella,‡,§ Leonardo Guidoni,‡,|| and Giovanni Ciccotti⊥,#

Dipartimento di Scienze Biochimiche "A. Rossi Fanelli", Università "La Sapienza", Piazzale Aldo Moro 5, 00185 Roma, Italy, Dipartimento di Fisica and CNISM Unit 1, Università "La Sapienza", Piazzale Aldo Moro 5, 00185 Roma, Italy, Dipartimento di Chimica, Ingegneria Chimica e Materiali, Università degli Studi dell'Aquila via Campo di Pile, 67100 L'Aquila, Italy, and Room 302b UCD-EMSC, School of Physics, University College Dublin, Belfield, Dublin 4, Ireland

Received: July 7, 2010; Revised Manuscript Received: September 30, 2010

Two indicators of the hydropathicity of small solutes are introduced and tested by molecular dynamics simulations. These indicators are defined as probabilities of the orientation of water molecules' dipoles and hydrogen bond vectors, conditional on a generalized distance from the solute suitable for arbitrarily shaped molecules. Using conditional probabilities, it is possible to distinguish features of the distributions in close proximity of the solute. These regions contain the most significant information on the hydration structure but cannot be adequately represented by using, as is usually done, joint distance−angle probability densities. Our calculations show that using our indicators a relative hydropathicity scale for the interesting test set of the quaternary ammonium cations can be roughly determined.

1. Introduction

Hydration structures around small solutes have been studied intensively, both theoretically and experimentally, in recent years.[1−5] The interest in this subject is due to the importance of hydration, often associated with hydrophobicity/hydrophilicity in biochemical processes.[6−9] Protein folding and biological self-assembly leading to micelles and membranes formation are important examples of chemical phenomena in which hydrophobicity plays a crucial role.[10−12]

The characteristics of the hydration of small solutes result from structural changes of the dynamical hydrogen bond network of the water molecules surrounding the solutes. Nonpolar (hydrophobic) solutes cause the exclusion of a few water centers from the water hydrogen bond network, leading to the formation of a small clathrate-like cavity around the solute. For small solutes the network is distorted without reduction of the number of hydrogen bonds. When the size of the solute increases, clathrate-like water cages are no longer stable, water molecules at the interface have dangling bonds and the total number of hydrogen bonds is reduced.[13] On the other hand, polar or charged (hydrophilic) solutes can form hydrogen bonds with water. This causes reorientation of the water molecules close to the solute, distorts their hydrogen bond pattern and decreases the average number of hydrogen bonds per water molecule.

Detailed insight into the hydration structure is provided by the geometrical analysis of the orientation of water molecules in the vicinity of the solute. The most indicative properties for this analysis are the distance from the solute, and dipole and hydrogen-bond (HB) orientations of the water molecules. For irregularly shaped molecules the solute−water distance must be defined appropriately (see section 2.3). Combined, these quantities can be used to construct distance-orientation distributions. Usually, the results of numerical simulations of hydration structures are presented in the form of joint-probability histograms.[14] This way of presentation has some disadvantages; namely, it diminishes or even completely hides the features of the probability for distances where it is relatively less likely to find a solvent molecule, for example, at small distances from the solute. This region, on the other hand, is the most affected by the presence of the solute. In this work, instead, we use conditional probability histograms. These histograms ensure that the angular distribution of dipoles or HB vectors for the regions of less frequent occurrence of water molecules are well represented, leading to a more detailed interpretation of the results and a deeper understanding of the solvation structure. In particular, we show that, using two appropriate conditional probabilities as indicators, it is possible to discriminate between hydrophilic and hydrophobic solutes and to construct a rough but informative scale of relative hydropathy of solutes with similar chemical characteristics. We apply this approach to study the hydration of the series of quaternary ammonium cations (QACs). This is a suitable test set for our purposes since the series starts from an essentially spherical molecule of well-defined hydrophilic character, the ammonium cation, and progresses to bigger molecules with more irregular shape and less defined hydropathy. These molecules also have a relevant biophysical role: QACs, in particular TEA^+ (see below), are often used in electrophysiology experiments to probe the gating and blocking mechanisms of ionic channels.[15] The nature of the molecular interactions between TEA^+ and the channel mouth is still debated and it has been extensively investigated by site directed mutagenesis,[16] X-ray crystallography,[17] and computer modeling.[18,19]

The paper is organized as follows. In section 2, we present the model of the system, with a detailed description of the solutes considered, and introduce the methods and observables used for the analysis. In section 3, we discuss the properties of

* To whom correspondence should be addressed. E-mail: wojciech.iwo.babiaczyk@roma1.infn.it.
† Dipartimento di Scienze Biochimiche, Università "La Sapienza".
‡ Dipartimento di Fisica, Università "La Sapienza".
§ CNISM Unit 1, Università "La Sapienza".
|| Università degli Studi dell'Aquila.
⊥ University College Dublin.
On leave from Dipartimento di Fisica and CNISM Unit 1, Università "La Sapienza", Piazzale Aldo Moro 5, 00185 Roma, Italy.

10.1021/jp106282w
Published on Web 10/28/2010

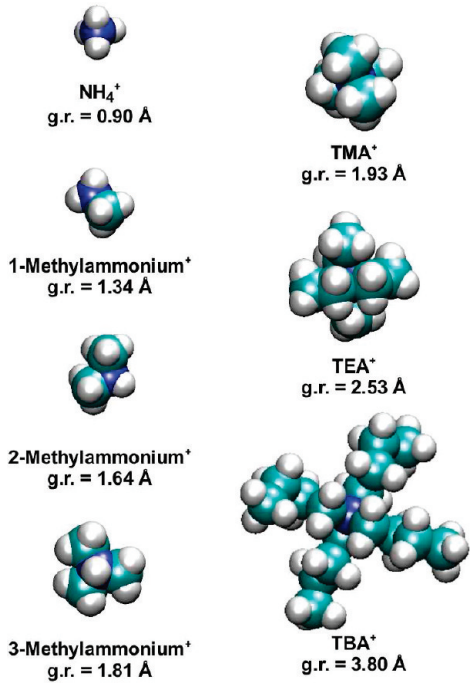

Figure 1. Quaternary ammonium cations. g.r. indicates the values of mean gyration radius. The ammonium cation (NH_4^+), with which the series begins is the smallest compound in the group. The next three compounds, mono-, di-, and trimethylammonium$^+$ cations, obtained by substitution of the subsequent hydrogen atoms with alkyl groups, are dipolar, but due to their larger size, the interaction with water/solubility is smaller. The last three solutes TMA^+, TEA^+, and TBA^+, obtained by substitution of all hydrogens with alkyl chains of increasing length (methyl, ethyl, and butyl), are slightly dipolar and the interaction with water is considerably weaker than for NH_4^+.

some reference compounds of well-defined hydrophobic/hydrophilic character, which will be used as a calibration for the QACs analysis, and show the advantages of conditional compared to joint probabilities on a typical example. In section 4 we present results for the QACs. The analysis discussed in this work depends on the choice of a particular water model. In all simulations reported we adopted the four point TIP4P water model. To validate this choice, we compared results obtained with this potential to those resulting from another commonly adopted interaction (TIP3P). Results for this comparison are discussed in the Appendix, where we show that TIP4P reproduces known experimental features of the hydration of given solutes more accurately.

2. The Model

For our analysis, we have chosen the following representatives of QACs series (Figure 1): We start with the ammonium cation followed by three protonated amines with increasing number of methyl substituents, the last being tetramethylammonium. Next, we vary the length of the substituent alkyl chains using ethyl and butyl groups. Thus, our series consists of the ammonium cation, NH_4^+, methylammonium, $NH_3CH_3^+$ ($1MA^+$), dimethylammonium, $NH_2(CH_3)_2^+$ ($2MA^+$), and trimethylammonium, $NH(CH_3)_3^+$ ($3MA^+$). They are followed by still positively charged but of yet smaller polarity tetramethylammonium, $N(CH_3)_4^+$ (TMA^+), tetraethylammonium, $N(C_2H_5)_4^+$-(TEA^+), and tetrabutylammonium, $N(C_4H_9)_4^+$ (TBA^+). As a solvent we use the four point rigid TIP4P[20] water model. To establish some reference hydration structures, we have also performed auxiliary simulations for pure water and solutes of

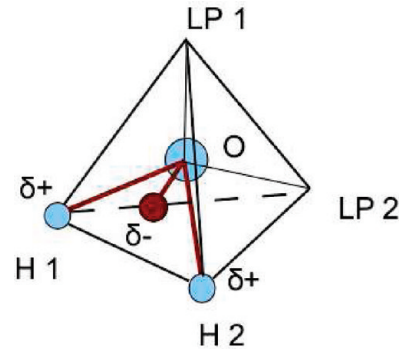

Figure 2. Tetrahedron representing a water molecule. The positions of the negative and positive partial charges of the TIP4P water model are indicated with deltas (the negative charge lies on the H1−O−H2 bisectrix) together with the directions of lone pairs (not included explicitly in the TIP4P model).

well-known hydrophobic/hydrophilic character, namely, hydrophilic K^+ and Cl^- ions and hydrophobic cyclohexane, C_6H_{12}.

2.1. MD Simulations. We performed molecular dynamics (MD) simulations using AMBER 9.[21] Each simulation consisted of a single solute molecule surrounded by TIP4P rigid water molecules in a cubic simulation box with imposed periodic boundary conditions. The number of water molecules and the size of the box varied with the size of the compound considered. In all cases, the quantity of surrounding water was sufficient to avoid problems with boundary conditions and to ensure an adequate sampling. Intramolecular interactions involving hydrogens were represented as rigid bonds and the SHAKE algorithm[22] was employed to solve the constrained dynamics for the degrees of freedom involved in these bonds. The other intramolecular interactions associated with bond stretching, bond angles, and dihedral angles, as well as all intermolecular Lennard-Jones and Coulomb interactions, were modeled using the "ff94" Amber force field.[23] Partial charges on the solutes were generated using the Austin Model 1 with bond charge corrections (AM1-BCC),[24,25] a semiempirical method that fits the partial charges by combining ab initio calculations with experimental data. Equilibration runs of 4 ns, in the constant temperature quasi-constant pressure ensemble, thermostated via Langevin dynamics[26] and barostated via the "weak coupling" method[27] were followed by production runs of 10 ns in the constant energy (*NVE*) ensemble. The particle mesh Ewald (PME) method was used to calculate the electrostatic interactions. In the equilibration runs the temperature was set to $T =$ 300 K and a time step of 1 fs was used in all simulations. Configurations were stored every 100 steps (0.1 ps). The histograms were collected at distance bin width of 0.05 Å, and angle bin width of 1°.

2.2. Observables. To characterize the local structure of water around different solutes, we have analyzed the orientation of water molecules with respect to the solute in its neighborhood.

A water molecule is usually represented as a tetrahedron (schematically shown in Figure 2): An sp^3-hybridized oxygen atom lies at its center and two hydrogens and two lone pairs constitute the four vertices. Due to such geometry a single water molecule can form up to four hydrogen bonds with other water molecules. Two of them will be called "active" (i.e., the reference water molecule shares its hydrogens), and two "passive" (i.e., the negative charge density of the lone pairs accepts hydrogens from neighboring water molecules). The ability to form hydrogen bonds with other water molecules gives rise to a HB network. When the propensity of a water molecule to form HB with other water molecules is analyzed, all vertices

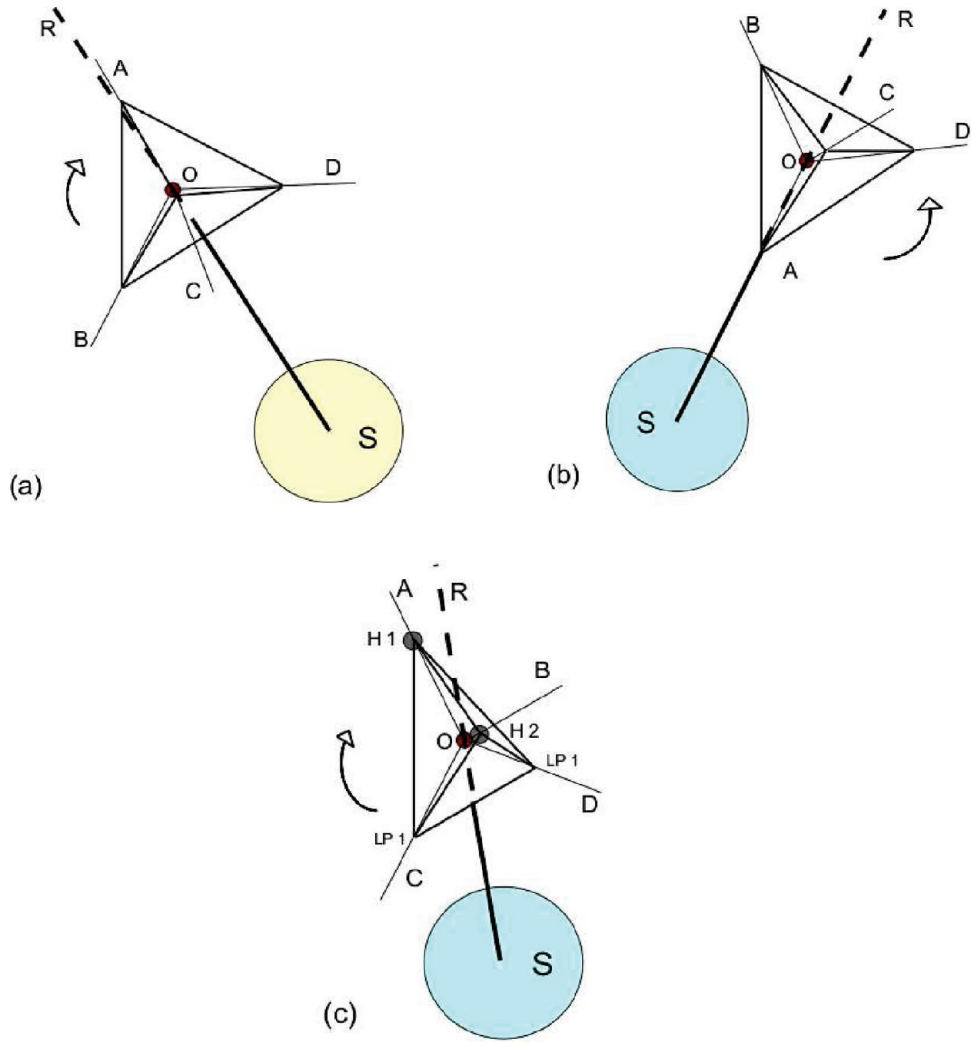

Figure 3. Most common orientations of a water molecule (tetrahedron) with respect to hydrophobic (a) and hydrophilic (b, c) solutes. Curved arrows show how to measure the angles. In the case of hydrophobic solutes (a), the water molecules try to maximize possibilities to form HBs with other water molecules, and the tetrahedron representing water opposes the solute with one of its facets. The angle between the A axis (from oxygen O in the center of the tetrahedron to the vertex A) and the line joining the solute with the water is $\angle(\mathrm{AOR}) \approx 0°$ and three remaining axis B, C, and D form $\angle(\mathrm{BOR}) \approx \angle(\mathrm{COR}) \approx \angle(\mathrm{DOR}) \approx 110°$. This orientation is called "clathrate-like". For the hydrophilic, not strongly charged solutes case (b), the tetrahedron points toward the solute with one of the vertices. The angles formed by the tetrahedron axis with respect to the vector joining the solute with the water's oxygen are: $\angle(\mathrm{AOR}) \approx 180°$, $\angle(\mathrm{BOR}) \approx \angle(\mathrm{COR}) \approx \angle(\mathrm{DOR}) \approx 70°$. This orientation is called "inverted". For strongly positively charged solutes, the angles formed by the axis of the tetrahedron containing the hydrogens with respect to the vector joining the solute with the water's oxygen are $\angle(\mathrm{AOR}) \approx \angle(\mathrm{BOR}) \approx 50°$ while for the axis with the LPs $\angle(\mathrm{COR}) \approx \angle(\mathrm{DOR}) \approx 125°$, respectively.

of the water tetrahedron can be treated as physically equivalent, as there is no need to distinguish between passive and active HB. At room temperature and atmospheric pressure, the thermal motion generates disorder so the network is dynamical with an average lifetime of the HB of the order of 1 ps.

In the presence of solutes, the number of HBs per water molecule can vary, depending on the polarity and size of the solutes. In general, two kinds of behavior can be observed. For relatively small and nonpolar neutral solute molecules (hydrophobic), the Coulombic interaction of hydration water molecules with bulk water molecules is stronger than the interaction with the solute that involves only van der Waals forces. Hence, the proximal water molecules are oriented so as to maximize the number of HBs with other water molecules. Geometrically, this situation is realized when one of the water tetrahedron's facets opposes the solute (see Figure 3a). In an idealized situation such orientation forms a regular cage around a solute. Indeed, at high pressure and low temperature, water forms such a cage, called a clathrate,[28−30] around a hydrophobic molecule. Due to this, the orientation of the proximal water molecules described above is called "clathrate-like".[31] A different behavior is expected for charged or polar solutes. In this case, water interacts with the solutes also via Coulomb forces. Depending on the charge and polarity of the solute, either one of the hydrogens or one of the lone pairs of the hydration water molecules is attracted toward it and one of the (possible) HBs with other water molecules is taken over by the solute. This is shown in Figure 3b. The tetrahedron is now facing the solute with one of the vertices. Such orientation of proximal water is called "inverted".[31] (The orientation of water shown in Figure 3c will be discussed later.)

In the following, the different orientations of the water tetrahedron resulting from the presence of hydrophobic/hydrophilic solutes will be characterized by combining the information provided by two probability densities. The first one is indicated as $P(R,\theta_h)$ and was introduced in ref 31. Here R is the modulus of the distance vector $\vec{R} = (x_O - x_s, y_O - y_s, z_O - z_s)$ defined as the vector joining the solute atom at $\vec{r}_s = (x_s, y_s, z_s)$ to the water molecule at $\vec{r}_O = (x_O, y_O, z_O)$ (see Figure 4 for definitions of these quantities). The origin of the vector is the solute's "backbone" (i.e., non-hydrogen) atom closest to the considered

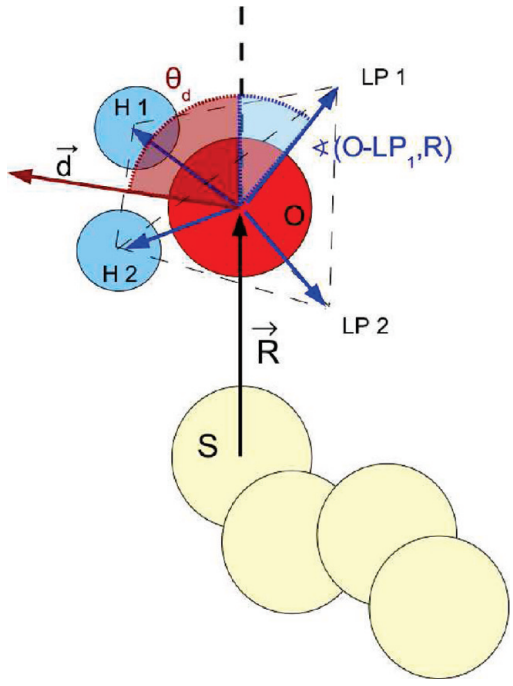

Figure 4. Definition of the vectors: The distance vector $\vec{R}$ (black) joins the solute atom "S" closest to the water's oxygen. The HB vectors (blue) originate from the water oxygen and end either at the hydrogen atoms (H1, H2 vectors) or at the LPs positions (LP1, LP2). The dipole vector $\vec{d}$ (red) is defined as the sum of the two O−H vectors. The orientation of the water molecule against the solute is determined via θ_d (red shaded angle) and four $\angle(\vec{V}_{HB_i},\vec{R})$ angles, where $HB_i = \{O-H_1, O-H_2, O-LP_1, O-LP_2\}$, corresponding, respectively, to the angle between $\vec{d}$ and $\vec{R}$, and the angle between the four HB vectors and $\vec{R}$. For clarity, only $\angle(\vec{V}_{O-LP_1},\vec{R})$ angle (blue shaded angle) is shown.

water molecule, while the end point is the oxygen atom of the water molecule. Two simplifications are introduced here. First, each atom is represented by the coordinates of the center of the corresponding point particle used in the simulation. Second, we considered only the positions of the oxygen atoms of the water molecules and those of the "backbone" solute's atoms, neglecting the positions of the hydrogen atoms in the solute. This is justified, as the center of mass of the residue formed by the hydrogens and the atom to which they are bound is situated in close proximity to the atom. The variable θ_h allows us to describe, partially, the orientation of a water molecule with respect to a solute. It is constructed as follows. First, we identify the four HB vectors in the water molecule: Two of them are the O−H vectors; the other two are the vectors joining the oxygen with the remaining two vertices of the tetrahedron (the LP directions). Second, we compute the angles that these vectors form with $\vec{R}$ using

$$\angle(\vec{V}_{HB_i},\vec{R}) = \arccos\left(\frac{\vec{R}\cdot\vec{V}_{HB_i}}{RV_{HB_i}}\right)$$

where $HB_i = \{O-H_1, O-H_2, O-LP_1, O-LP_2\}$. The variable θ_h is defined as the value of *any* one of these angles. In other words, $P(R,\theta_h)\,dR\,d\theta_h$ is the probability of the event that *any* of the $\angle(\vec{V}_{HB_i},\vec{R})$ angles takes a value between θ_h and $\theta_h + d\theta_h$ and that there is a water molecule at a distance between R and $R + dR$ from the solute. Note that, in the TIP4P model we adopt, the HB axis related to the lone pairs does not have physical meaning since the LP partial charges do not appear in the potential (see Figure 2 for the location of the partial charges in TIP4P water). To us, these axes are indicators of the preferred bonding directions of the water molecules and of their propensity to form HBs. While these directions are important, it has been argued[9] that the electron-density distribution shows a single broad maximum on the water's oxygen atom. Thus, for the case of stronger positive charge of the solute, it may happen that the water molecule points toward the solute with the oxygen atom, while the two hydrogens are directed outward, as shown in Figure 3c.

The shape of the probability $P(R,\theta_h)$ discriminates three situations (see also the caption of Figure 3):

1. For hydrophobic solutes water is oriented so as to maximize the possibility to form HBs with other water molecules and the water tetrahedron opposes the solute with one of its facets (see Figure 3a). This results in two peaks in the $P(R,\theta_h)$ probability located approximately at $\theta_{h1} \approx 0°$ (this peak has multiplicity one as it arises from angle AOR in Figure 3a) and $\theta_{h2} \approx 110°$ (multiplicity three as it is due to the angles BOR, COR, and DOR in Figure 3a).
2. For hydrophilic solutes of negative or positive (weak) charge the tetrahedron points toward the solute with one of the vertices (see Figure 3b). Irrespective of the sign of the charge, the probability $P(R,\theta_h)$ has two peaks located approximately at $\theta_{h3} \approx 180°$ (this peak has multiplicity one as it arises from angle AOR in Figure 3b) and $\theta_{h4} \approx 70°$ (multiplicity three as it is due to the angles BOR, COR, and DOR in Figure 3b).
3. For hydrophilic solutes of strong positive charge, the water molecule points toward the solute with the oxygen atom (see Figure 3c). In this case, $P(R,\theta_h)$ has two peaks located approximately at $\theta_{h5} \approx 50°$ (multiplicity two as it is due to the angles AOR and BOR in Figure 3c) and $\theta_{h6} \approx 125°$ (this peak also has multiplicity two as it is due to the angles COR and DOR in Figure 3c).

The description of the orientation of the water tetrahedron obtained from the probability described above is purely geometrical and thus insensitive to a relevant physical characteristic of the solute. Since we assume that all vertices are equivalent, we cannot discriminate among the solvation structure induced by positively or negatively charged solutes. This information can, however, be recovered thanks to the second probability that we now introduce, $P(R,\theta_d)$, where

$$\theta_d = \arccos\left(\frac{\vec{R}\cdot\vec{d}}{Rd}\right)$$

is the tilt angle describing the water's dipole orientation with respect to the solute. In the equation above, $\vec{d}$ is the water dipole, defined as $\vec{d} = \vec{V}_{H_1-O} + \vec{V}_{H_2-O}$, with $\vec{V}_{H_i-O} = (x_{H_i} - x_O, y_{H_i} - y_O, z_{H_i} - z_O)$, $i = 1, 2$. The sum is not normalized as we are interested only in the relative orientation of the vectors. Figure 5, in particular the caption, illustrates how the orientation of the dipole vectors of proximal water molecules provides the needed information about the solute's charge (Figure 5a) and, in the case of hydrophobic solutes, specifies the direction of the O−H bonds (Figure 5b). The shape of the probability $P(R,\theta_d)$ allows us to discriminate three situations:

1. For ideal positively charged hydrophilic solutes, the probability $P(R,\theta_d)$ has a single peak centered at $\theta_{d1} \approx 75°$ (see Figure 5a). In TIP4P water the negative charge is more localized than the one found in ab initio calcula-

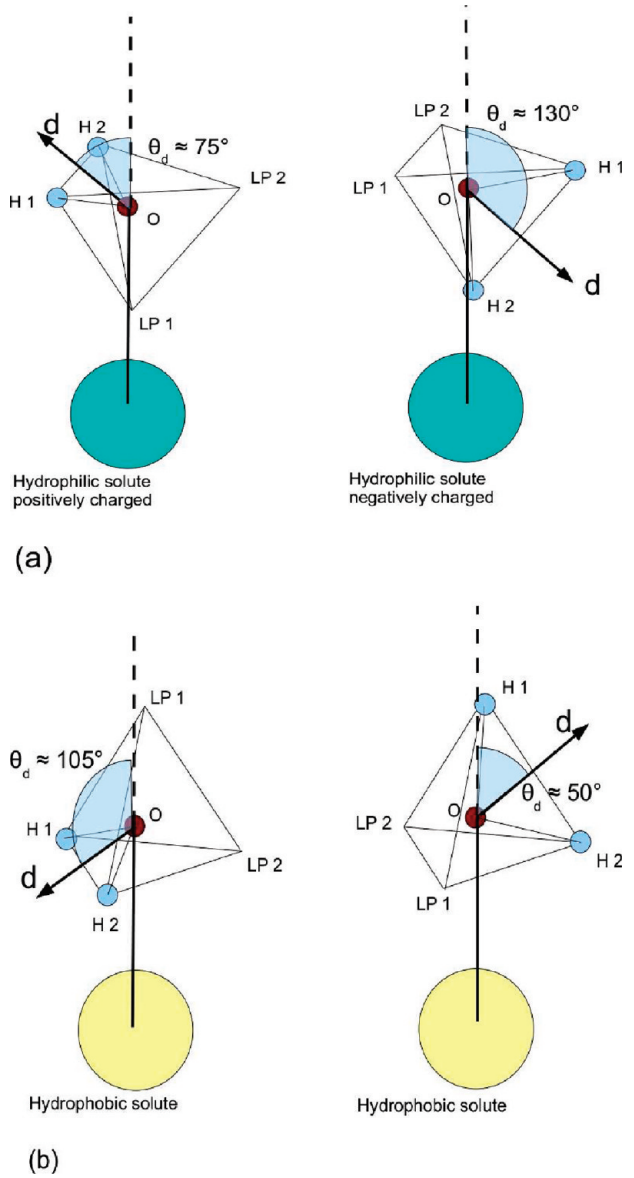

Figure 5. Complementary information provided by the orientation of the dipole vector of the water molecule. In (a) the orientation of water with respect to hydrophilic solutes of different sign charge is shown. With the θ_d angles it is possible to distinguish between different characters of charged solutes. In the ideal case, $\theta_d \approx 75°$ for cations, and $\theta_d \approx 130°$ for anions. In (b) the different possible positions of the water molecule are shown in the case of a hydrophobic solute. As they are physically equivalent, both values of $\theta_d \approx 105°$ and 50° should appear as peaks in the θ_d distribution.

tions. This modifies the interactions with respect to the "ideal" case and smears the peak between 0° and 60°.

2. For negatively charged hydrophilic solutes, the probability $P(R,\theta_d)$ has a single peak centered at $\theta_{d2} \approx 130°$ (see Figure 5a).
3. For hydrophobic solutes, the probability shows two peaks at $\theta_{d3} \approx 105°$ and $\theta_{d4} \approx 50°$ corresponding to different, but physically equivalent, hydrogen positions with respect to the solute (see Figure 5b).

In sections 3 and 4, we illustrate how $P(\theta_h|R)$ and $P(\theta_d|R)$ can be used together to characterize the hydration structures of different solutes.

2.3. Conditional Probabilities Formulation. The $P(R,\theta_\alpha)$, $\alpha = d, h$, described in the previous section is the *joint* probability density to find a water molecule at a distance R *and* oriented at angle θ_α. Unfortunately, using the joint probability distribution, the features in the regions of lower distance probability density, e.g., in the vicinity of the solute, are diminished or even completely washed out. Instead, one can use the *conditional* probability distribution, where the probability of finding a molecule oriented at an angle θ_α, *given* the distance R is considered. This probability emphasizes the features in the regions of less frequent occurrence of water molecules. To construct the conditional distribution, the joint distribution $P(R,\theta_\alpha)$ has to be divided by the marginal probability, $P(R)$, i.e., $P(\theta_\alpha|R) = P(R,\theta_\alpha)/P(R)$. Determining $P(R)$, or $P(R,\theta_\alpha)$, for solutes of arbitrary shape is nontrivial, since an appropriate definition of the distance vector $\vec{R}$ must be given. Using a probability based on the traditional definition of Euclidean distance with respect to the center of mass of the solute molecule, accurate information about the surrounding solvent structure can be obtained only for spherically shaped molecules. For molecules of arbitrary shape it is more useful to account for the morphology of the solute, and in particular of the "surface" that it exposes to the solvent, by modyfing the definition of distance. Consider the water molecule at position $\vec{r}_i$: Its distance from the solute is defined as $D_i = \min_s|\vec{r}_i - \vec{r}_s|$, where $\vec{r}_s$ is the position of the "backbone" atom s of the solute. This automatically associates each solvent molecule with the closest solute's non-hydrogen atom. The probability to find a water molecule at a distance R from the solute can then be computed, for example, along an MD trajectory of duration τ, as

$$P(R) = \lim_{\tau\to\infty} \frac{1}{\tau N_w} \int_0^\tau dt \sum_{i=1}^{N_w} \delta(R - D_i(t))$$

where N_w is the number of water molecules. The procedure described above allows us to construct probability density functions that display a well-developed shell structure, for arbitrary shape of the molecule and to extract from them useful structural properties like the width of the hydration shells or the coordination number. The same definition was employed for the distance in the joint probability density. The results of our simulations are 2D histograms of the conditional probability distribution of the angles θ_α, given a certain distance. The histogram $h(R,\theta_\alpha)$ is the two-dimensional array in which the distance R and θ_α are collected. The probability density $P(R,\theta_\alpha)$ is obtained from

$$P(R,\theta_\alpha) = \frac{h(R,\theta_\alpha)}{\mathcal{N}}$$

where the normalization factor is

$$\mathcal{N} = \int dR\, d\theta_\alpha\, R^2 \sin(\theta_\alpha)\, h(R,\theta_\alpha)$$

The conditional distribution reads

$$P(\theta_\alpha|R) = \frac{P(R,\theta_\alpha)}{P(R)}$$

where the marginal probability is computed as

$$P(R) = \frac{\int d\theta_\alpha \sin(\theta_\alpha)\, h(R,\theta_\alpha)}{\mathcal{N}}$$

A comparison of the results that can be obtained with the joint and conditional probability densities is shown at the end of the next section.

3. Hydration of Solutes of Known Hydrophobic/Hydrophilic Character

3.1. Water Structure. The structure of water is determined by the existence of hydrogen bonds between water molecules. In Figure 6, we show a snapshot of part of the hydrogen bond structure of bulk TIP4P water. The active HBs (blue dotted lines) are formed by molecule 1 with molecules 2 and 3 (that "see" the positive charge of the hydrogens in molecule 1). The passive HBs are formed with 4 and 5 (that "see" the negative charge on 1). The relative orientation of the water tetrahedrons is the "inverted" one (compare Figures 3b and 5a). If we consider the $P(\theta_h|R)$ for the reference molecule 1, the configuration of surrounding molecules results in two peaks centered at about 70 and 180° in the first hydration shell (1HS), as shown in Figure 7b (we define the kth hydration shell, kHS, as the region between minima k and $k + 1$ of the $P(R)$). In the ideal case, with the surrounding water tetrahedron pointing precisely toward the reference water oxygen, the 70° peak should be 3 times more intense than the 180° one. As explained in more detail in the caption of Figure 3 there are, in fact, three axes of the tetrahedron oriented at the angle of 70° and only one at 180°. However, due to thermal motion, both peaks are broadened, more so the 70° peak which is, in fact, a superposition of three very close peaks. This is so because when the tetrahedron does not lie exactly along one of its axis, the three protruding axes never form identical angles with the distance vector due to thermal noise. As discussed earlier, the dipole orientations for the same tetrahedral geometry can vary. Indeed, due to the simultaneous presence of active and passive hydrogen bonds, $P(\theta_d|R)$, shown in Figure 7a, has two peaks in the 1HS: A broad peak extending from 0° to 60° and a narrow one at 130°. The peak at 130° corresponds to the passive HBs between reference and surrounding water molecules (this happens when the reference molecule HB is pointing toward H), while the smeared one is due to the active HBs (this happens when the reference molecule HB is pointing toward LP). As shown in Figure 5a, for active HBs, the angle between the dipole and distance vectors should be about 75°, with one of the lone pairs pointing exactly toward the reference molecule (see also Figure 3b). In our simulations, however, as the TIP4P water model does not include the lone pairs partial charges, the geometry of the hydrogen bonding is a compromise between the tendency of water molecule to form as many HBs as possible with other molecules (optimal geometry) and the location of a single-point negative partial charge on the oxygen atom, which leads more likely to the situation shown in Figure 3c. As a result, the maximum of the peak is at about 45°, and the peak extends from 0° to about 60°. In the case of passive HB, the situation is simpler, as the hydrogen atoms of the surrounding molecules point directly toward the oxygen atom of the reference water molecule. This corresponds to the narrow peak centered at about 130°. Toward the second hydration shell (2HS), the configuration of the water molecules first becomes "clathrate-like", then again "inverted" at about twice the position of the 1HS center. This is due to the geometric constraints imposed on farther water by the molecules in the 1HS. The molecules in the center of the 2HS, which are closer to the reference molecule than twice the distance to the center of 1HS, do not show any particular tendency to be either in "inverted" or "clathrate-like" configuration. The situation can be clearly seen in the θ_h distribution in Figure 7b, where the "clathrate-like", 0° and 130° peaks, at the external boundary of the 1HS are split into three ridges, converging to "inverted" 75° and 180° peaks at about 5.5 Å, at the 2HS border. The complementary information from the dipoles orientation distribution shows two peaks centered at about 80° and 180° formed behind the 1HS and converging into one 130° peak at a distance of about 5.5 Å from the reference molecule. Also a 0° peak formation can be observed in the center of 2HS, which is wiped out at larger distances. As bulk water ordering is not radially symmetric, the hydration pattern is blurred for larger distances.

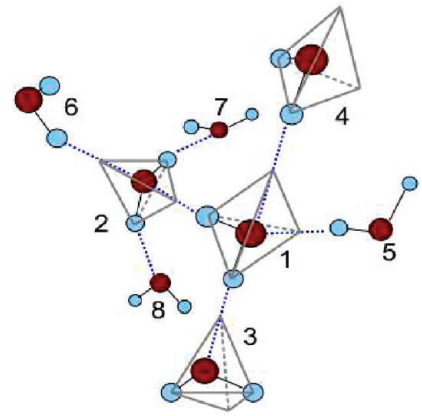

Figure 6. Snapshot of a region in bulk water. Hydrogen bonds between water molecules are depicted in blue dashed lines. Focusing on molecule 1 as our solute, bonds 1−2 and 1−3 are active, while 1−4 and 1−5 are passive HBs.

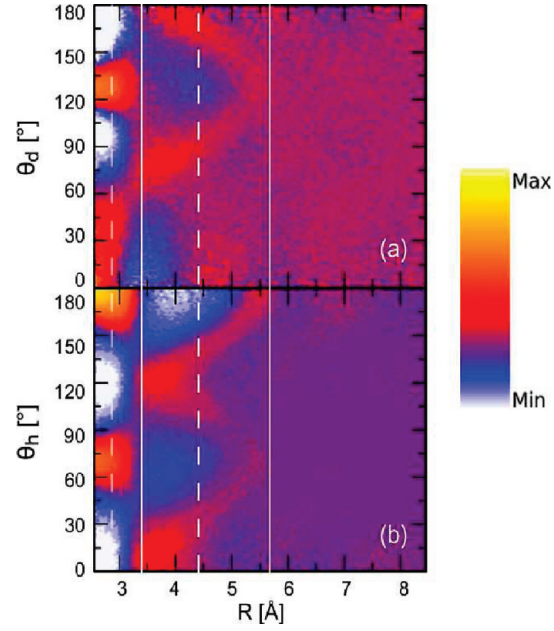

Figure 7. Bulk water: conditional distribution of θ_d (a) and θ_h (b) angles, given the distance R. Here and in all histograms shown in the following, the white solid lines indicate the limits and the dashed lines the centers of the HSs (see text for details). (a) $P(\theta_d|R)$: The broad peak extending from 0° to about 60° and the narrow peak centered at ∼130° are characteristic of the "inverted" orientation. (b) $P(\theta_h|R)$: The 75° and 180° peaks are also typical of the "inverted" orientation. The "clathrate-like" peaks in the 2HS are induced by the orientation of water in the 1HS (see text).

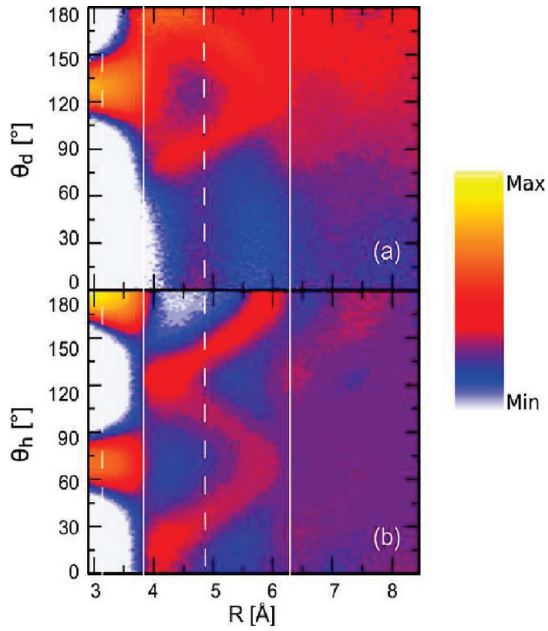

Figure 8. Cl^- anion: $P(\theta_d|R)$ (a) and $P(\theta_h|R)$ (b). The strong peak at about 130° in the θ_d distribution (a) results from $Cl^-\cdots(H\text{---}O)_{surr}$ bonds. The 75° and 180° peaks in the θ_h distribution in the 1HS (b) confirm this "inverted" orientation. For larger distances, the orientation changes to bulk water configuration.

3.2. Hydrophiles and Hydrophobes. Hydrophiles can be most generally described as substances to which water molecules can transiently bind. This can happen via an active HB, for example, when water acts as a hydrogen donor toward anions or anionic groups of complex molecules ($O-H\cdots ion^-$), or via a passive HB, for example, when water acts as acceptor of the hydrogen donated by a positively charged solute that contains hydrogen ($ion-H^+\cdots O-H$). Somewhat improperly, since in this case simple electrostatic interactions are involved, we shall also refer to the bond formed by a cation that does not contain hydrogens with the negatively charged oxygen atom on the water molecule as a passive HB ($ion^+\cdots O-H$).

Let us consider the case of a single Cl^- solute. Our results for the dipoles and HB vectors orientation distributions are shown in Figure 8a,b, respectively. In the θ_d distribution a narrow peak at 130° can be observed in the 1HS; two ridges, beginning at about 80° and 180° in the region between 1 and 2 HS and converging to a single 130° peak (ridge) at about twice the distance from solute to 1HS, are also visible. This part of the plot is very similar to the upper part of the analogous plot for pure water, as one would expect, since it describes the formation of the same type of HB. Note, however, that the lower part of the histogram is different from Figure 7 since in this case no passive HBs can be formed. The whole θ_h distribution is very similar to that for the pure water system. Again, this is to be expected, because, as we mentioned before, the characterization of the orientation of the water molecule tetrahedron with respect to the solute (or the reference water molecule) does not differentiate between different HB types. The enhancement of the features in the 2HS with respect to the histogram for bulk water can be attributed to the absence of the passive HBs with the solute.

Let us now move to the probability densities for a single K^+ solute shown in panels a and b of Figure 9 (panels c and d will be discussed in the Appendix). The θ_d distribution plot shows the broad maximum extending from 0° to 60° in the 1HS, which is also present in the lower part of the θ_d plot for pure water, as the solvent water forms the passive HB with the K^+ solute. When compared to the distribution for bulk water (see Figure 7a), an enhancement of the features at larger distances similar to the one observed for Cl^- (see Figure 8a) can be seen in the lower part of the distribution, this time induced by the lack of competition from the active HBs with the solute. The θ_h distribution is again very similar to the one for bulk water.

Hydrophobic solutes are repelled from water. They are neutral nonpolar molecules, and thus water does not form any kind of hydrogen bond with them. Let us consider as an example a single cyclohexane molecule in water. Our analysis for this molecule is shown in Figure 10. Let us concentrate for the moment on panels c and d of the figure that represent the

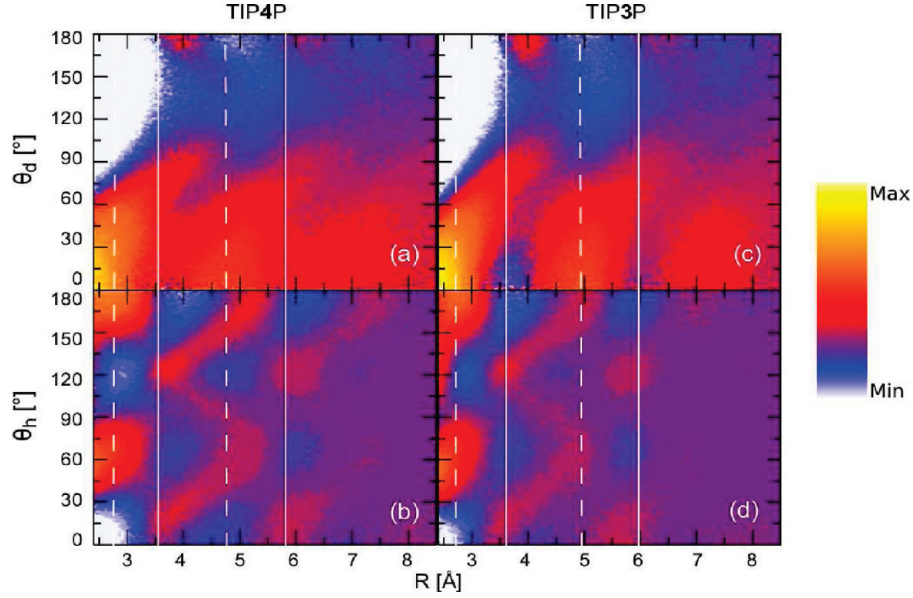

Figure 9. K^+ cation: conditional distribution of θ_d and θ_h for TIP4P (a, b) and TIP3P (c, d) solution, respectively. The smeared peak between 0° and 60°, characteristic of passive HB-type bonding between solvent water molecules and K^+, can be observed in the 1HS in the θ_d distribution of both models. The structure of the θ_h distribution is clearly "inverted" in both cases, resulting in the 75° and 180° peaks in the 1HS. In the TIP3P plot (d), a spurious peak at 130° is observed. This peak corresponds to the orientation of solvent water molecules described in Figure 3c and is an artifact of the model, as experiments show that such a peak exists only for charge of the solute greater than 1 (see Appendix for details).

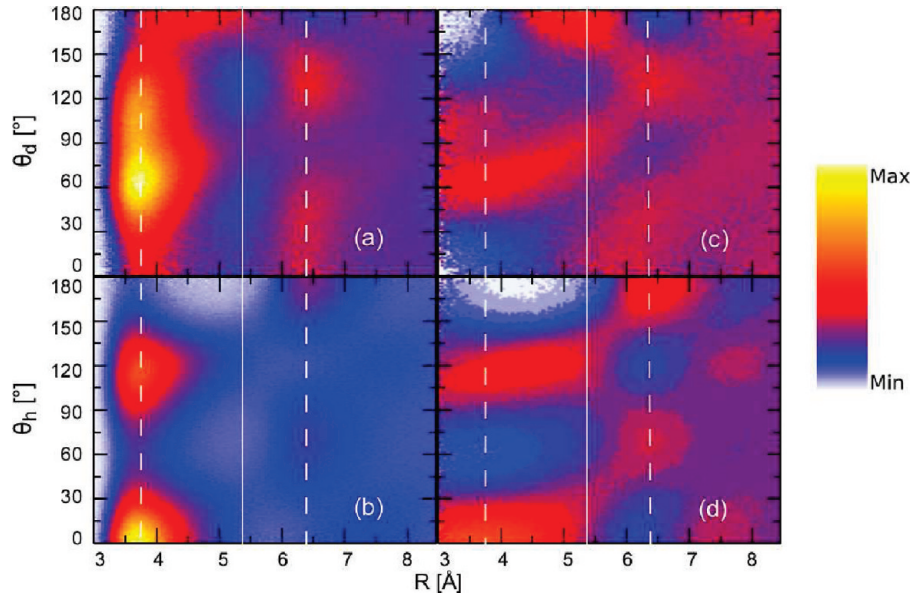

Figure 10. Cyclohexane: joint probability distributions $P(R,\theta_d)$ (a) and $P(R,\theta_h)$ (b) and conditional probability distributions $P(\theta_d|R)$ (c) and $P(\theta_h|R)$ (d), respectively. The most striking differences between the distributions are the lack of structures for $R < 3.5$ Å in the JPDs and the different widths of the peaks in the border region between the centers of the 1HS and the 2HS (see comments in the text).

conditional probability density $P(\theta_\alpha|R)$ (panels a and b will be discussed in the next subsection). In panel c, we can see a broad peak in the θ_d distribution, which extends through the whole 1HS, tending to about 60° at the center of the shell, accompanied by a peak at 100° in the vicinity of the molecule. This indicates that the water tetrahedron is oriented with its basis roughly tangential to the solute (compare Figure 5b). This situation results from the competition between the favorable interaction between water molecules due to electrostatic forces and the weak interaction between solvent water and solute, limited to van der Waals forces only. The commonly accepted justification for such orientation of solvent water molecules is the fact that water tends to create a "clathrate-like" cavity in which the solute is trapped. The θ_h distribution is shown in Figure 10d. The two wide peaks centered at 0° and about 125° in the 1HS and the elongated, in comparison to the region for hydrophiles, intermediate region confirm the "clathrate-like" orientation of solvent water. In the θ_d distribution (see Figure 10c) at the beginning of the 2HS the features observed for bulk water appear, namely, the characteristic 80° and 180° peaks converging to a single 130° peak and in the θ_h distribution (see Figure 10d) the three ridges converging to "inverted" orientation 75° and 180° peaks. These peaks positions are shifted when compared to those for pure water, since for pure water the orientations of the molecules in the 2HS are due exclusively to interactions with waters in the 1HS, while in the presence of a solute the positions of the peaks reflect the water−solute interactions.

3.3. Conditional versus Joint Probability Density Plots. In Figure 10 we compare the joint and conditional probability densities (JPD and CPD, respectively) for the hydrophobic cyclohexane solute described above. $P(R,\theta_d)$ is shown in panel a, and $P(R,\theta_h)$ in panel b, while panels c and d refer to the CPD. Both the JPD plots do not show any features in close proximity of the solute, and $P(R,\theta_h)$ is essentially flat for $R >$ 4.5 Å. This lack of features can be explained by looking at the marginal probability $P(R)$ for this solute, shown in Figure 11. The marginal goes to zero in the vicinity of the solute reflecting the excluded volume effect that dominates the behavior of the JPD in this region. For larger distances the JPD is dominated by the maximum of the 1HS and cannot adequately resolve the

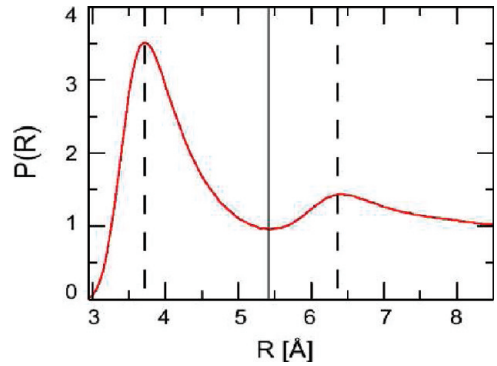

Figure 11. Cyclohexane: Marginal probability distribution $P(R)$.

water orientation for all relevant values of the distance. On the contrary, the CPD remains finite for shorter distances and provides a signal consistent with the discussion of the water orientation presented in section 2.2. Furthermore, the CPD shows peaks of comparable intensities for distances corresponding to the first and second maxima of the marginal probability. The ratio defining the conditional probability also enhances the signal in the regions between the maxima of the marginal probability, proving to be a sentitive probe throughout the first two hydration shells. The different behavior of the joint and conditional probabilities in the region between the maximum and the boundary between the 1HS and 2HS is particularly important: The features shown by the CPD for θ_h in this region, absent in the JPD, can be used as indicators of hydropathicity. As discussed in the following (see also Figures 8 and 10), these features are enhanced for hydrophobic and reduced for hydrophilic solutes.

4. Hydration of Quaternary Ammonium Cations

The ammonium cation series starts with the ammonium ion NH_4^+. In NH_4^+, four hydrogen atoms form a tetrahedron around a sp^3-hybridized nitrogen. In our analysis the ammonium cation resembles alkali metals cations, e.g., K^+, and therefore the hydration of this molecule should be very similar to the hydration of K^+. Indeed, the results (see the first column of

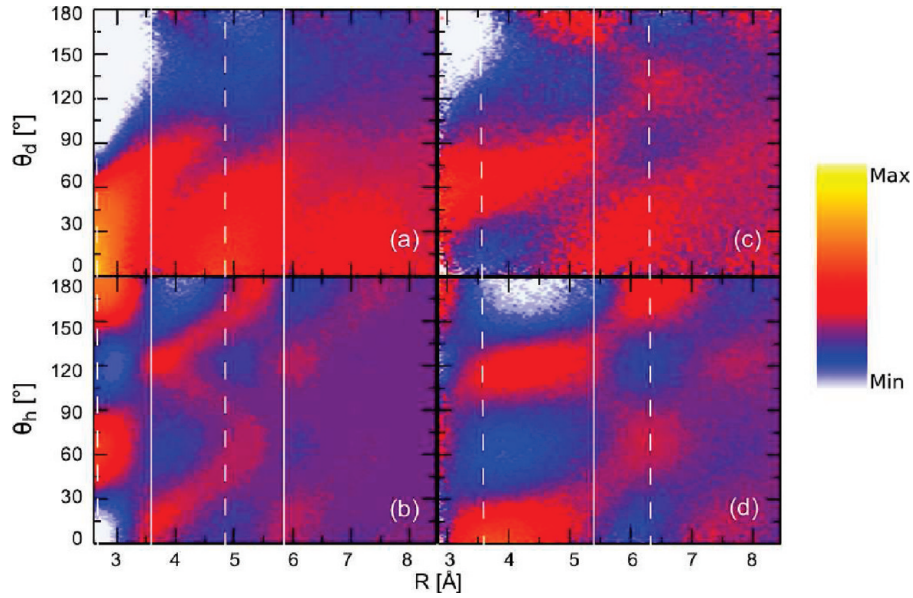

Figure 12. Ammonium (the smallest of QACs, left panel) and TBA^+ (the largest one, right panel) cations: $P(\theta_d|R)$ and $P(\theta_h|R)$ are shown on the top and bottom parts of figure, respectively. The smeared peak from 0° to about 60° in the $P(\theta_d|R)$ for ammonium (a), characteristic of the hydrophilic behavior of the water molecules in the 1HS, becomes more centered at about 60° in the $P(\theta_d|R)$ for TBA^+ (c). The corresponding maximum in the center of the 2HS present for ammonium is smeared and diminished for TBA^+. On the other hand, the "inverted" peaks at 75° and 180° in the $P(\theta_h|R)$ present in the NH_4^+ system (b) are almost vanished for the TBA^+ (d), while the narrow peaks at 0° and 110° at the border of the 1HS for ammonium, corresponding to the "clathrate-like" orientation of solvent water, are broadened and shifted toward the center of the 1HS for the TBA^+.

Figure 12) are nearly identical to those for the K^+ system. All the features visible for K^+ are repeated for the ammonium cation, and thus the detailed analysis presented for K^+ is valid also for this case. This means that the QACs series begins with a purely hydrophilic molecule highly soluble in water. The last molecule in our QACs series is TBA^+, in which all hydrogens of NH_4^+ are substituted with butyl (C_4H_9) groups. This is the largest of the solutes considered in our work. Despite the fact that TBA^+ is a cation, its hydration structure is similar to that of hydrophobic solutes. In Figure 12, we compare the conditional distributions for θ_d and θ_h for ammonium and TBA^+. The plots for TBA^+ are almost identical to the cyclohexane plots. This means that the water molecules surrounding the TBA^+ solute tend to form a clathrate-like cavity around it. In fact, the cations from this family of compunds are called "hydrophobic cations", a fact fully supported by experimental evidence[32] and revealed also by our analysis. The histograms, however, can also capture small differences with fully hydrophobic compounds, which cannot be observed in experiment. The most prominent is the absence of the 100° peak in the 1HS in the θ_d distribution. A slight shift toward lower values of θ_d and faint traces of the corresponding "inverted" 70° and 180° peaks in the θ_h distribution in the very close neighborhood of the solute are also present. Note that these features would not be visible in the joint probability density, as illustrated in section 3.3. These features are a consequence of the cationic character of the solute and of the fact that its charge is delocalized. This weakens the intensity of the Coulomb interaction between the solute and individual water molecules, which are then more strongly influenced by the other water molecules. The hydropathicity of the remaining compounds of the QACs series lies between the hydrophilic and hydrophobic extremes. As can be expected, with increasing number and elongation of the alkyl substituents the hydrophobic character of the solutes becomes dominant. This is signaled in the upper row of Figure 13 by the progressive disappearance of the features of the dipoles distribution at larger distances and by the narrowing of the peak in the 1HS whose center shifts toward 60°. An even more evident indication of the change in hydropathicity is provided by the changes in the structures in $P(\theta_h|R)$ shown in the second row of the figure. The intense narrow peaks centered at 60° and 180° in the 1HS, signatures of strong hydrophilicity, diminish in intensity as we progress along the series and have almost completely disappeared at the end. Furthermore, the narrow 0° and 130° peaks in the ridges at about 4 Å smoothly increase their width with increasing hydrophobicity. As can be appreciated better from Figure 12, the localization of these peaks also changes from the border of the 1HS and 2HS (hydrophilic solute) to well inside the 1HS (hydrophobic case).

5. Concluding Remarks

In this work we explored the possibility of characterizing the relative hydropathicity of different solutes via the geometrical analysis of the orientation of neighboring solvent water molecules. We proposed to use as indicators two conditional probabilities: The water dipole's vector angle distribution, given the distance between solute and water molecules and the distribution of the HB vectors orientations, given the same distance. The possibility to characterize hydropathicity based on these indicators was tested on a set of small solutes belonging to the quaternary ammonium cations. QACs were chosen because the character of the subsequent set members changes from purely hydrophilic to hydrophobic. To analyze the results, two important tools were used. First we introduced a suitable definition of distance when calculating the probability densities. This definition enables the appropriate exploration of the hydration shells of arbitrarily shaped molecules and, hence, could be applied to all molecules in the QACs series. Second, we used conditional probability densities, rather than joint probabilities. This choice emphasizes features in regions close to the solute, particularly in the first two hydration shells, where the behavior of water is crucial for determining the hydrophilicity/hydrophobicity. Our results show that we can easily

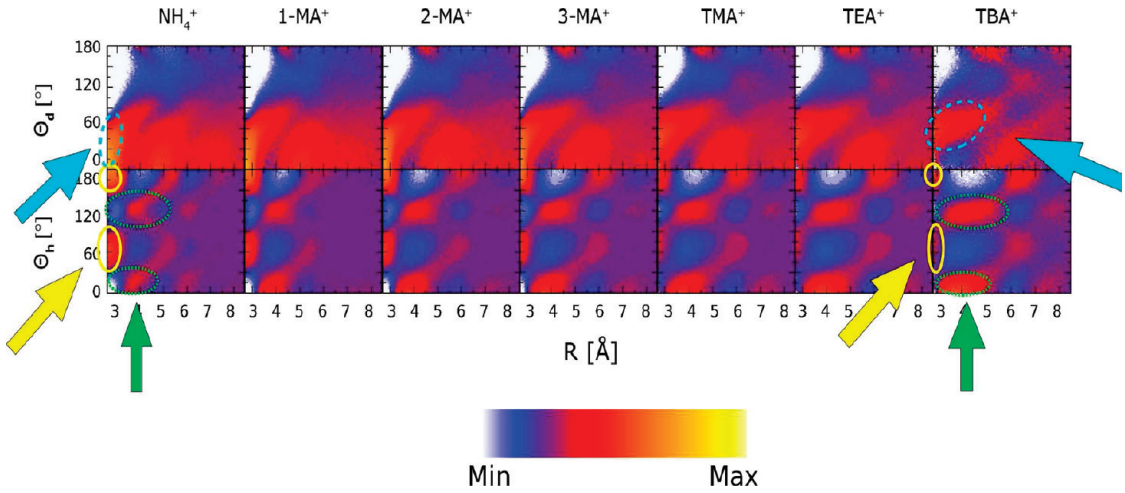

Figure 13. $P(\theta_d|R)$ (top) and $P(\theta_h|R)$ (bottom) for the QACs series. Starting from the left, the results for NH_4^+ system are shown, then for mono-, di-, trimethylammonium and TMA^+, TEA^+, and TBA^+ cations, respectively. Blue arrows in the upper panels indicate the shift of the peak in θ_d distribution corresponding to the change of the dipoles' orientation. Yellow arrows in the bottom panels indicate the diminishing contribution from "inverted" orientation 75° and 180° peaks in the 1HS. Vertical green arrows point to the increase of the intensity of the "clathrate-like" 0° and 125° peaks in the θ_h distribution as the hydrophobicity increases. The ellipses are just guides for the eye.

discriminate highly hydrophobic or hydrophilic cases. The definition of a fine scale for intermediate cases is less straightforward, but some features of the conditional probabilities can serve as indicative markers. In particular, the intensity and width of two peaks in $P(\theta_h|R)$ change quite smoothly with the character of the solute. These peaks are narrow and localized at the boundary between the 1HS and the 2HS for hydrophilic solutes and become progressively broader and shifted toward the center of the 1HS as the hydrophobicity of the solute increases. While at this stage this is not enough to establish a quantitative scale of relative hydropathicity, the structure and location of these peaks do provide interesting information and may be used in future work as the starting point of a more precise characterization of the properties of different solutes. As a final remark, the outcome of a hydropathicity analysis based on our indicators (or on any scale that employs calculations) will depend on the choice of the potentials adopted in the simulation. In the Appendix, we examined the effect of using two different rigid water models, TIP3P and TIP4P, and concluded that the latter is the more reliable. The choice of the potential describing the solute and the solute−water interactions can also affect the results of the analysis. In this work, we adopted the so-called "second generation" Amber ff94 force-field for reasons of computational ease and efficiency. Of course, other choices are possible (for example, simulations based on optimized potentials for liquids,[33] or ab initio simulations). However, the agreement with experiments and ab initio calculations of the trends for the hydrophobicity of our series with charge and size reported in the Appendix encourage us to believe that the choice we made is reasonable. Furthermore, while the potentials will affect the specific outcome of a given calculation, we believe that different choices will not affect the general framework and the conclusions of this work.

Acknowledgment. This work was partially supported by Award No. KUK-I1-012-43 made by King Abdullah University of Science and Technology (KAUST). G.C. acknowledges financial support from Science Foundations of Ireland (SFI) through the PI Grant 08/IN.1/I1869. L.G. acknowledges funding provided by the European Research Council project n. 240624 and computer resources from CASPUR grant no. std09-332.

Appendix: Transferability of TIP4P/TIP3P Water Models

The choice of the water model used as solvent is crucial to get the relevant hydration structures. TIP4P four point water model is surely one of the best to describe pure water in terms of structure, dynamics, and phase transitions. When performing an MD simulation of ions in water solution, however, one has to pay attention to the fact that, even though one part of the force-field parameters (water in this case) is the best, there is also the solute part, and all the parameters should be consistent with each other. The Lennard-Jones parameters used in the simulations with AMBER 1994 force field are extracted by fitting thermodynamic experimental data (solvation free energies) using TIP3P specific water model. At first, then, it seems that the compulsory choice is the TIP3P model. In view of recent research, however, this is not necessarily the case. An extended comparison of small-molecule hydration free energies for TIP3P/TIP4P water models with partial charges obtained by various methods (including AM1-BCC used in this work) is given in ref 34. The results for TIP3P and TIP4P indicate that both solvents do not reproduce the experimental values exactly. However, using TIP4P with AM1-BCC calculation of the partial charges, the free energy of hydration of diethylamine, which is a compound very similar to our QACs, is closer to the experiment than the TIP3P result which strongly underestimates the value. As for alkali and halide ions parameters, an extended review is given in ref 35. In this case the disagreement with reference values of the free energies of hydration of K^+ ion and Cl^- is a bit smaller for TIP3P (about 5% difference) than for TIP4P (about 10% difference). The comparison for single water−ion binding, on the other hand, shows that the reference results are reproduced equally well by both models. The disagreement for K^+ is 0 and 0.76% for TIP3P and TIP4P, respectively, and for Cl^- 2.9 and 2.2% for TIP3P and TIP4P, respectively. The radii of the first hydration shell are shown to be slightly closer to reference values for TIP4P water.

In Figure 9, we compare conditional probabilities computed with TIP3P and TIP4P water models for K^+. Our results confirm the better geometrical performance of TIP4P water. The difference in dipoles' orientation distributions (see Figure 9a,c), is almost negligible. In HB-vectors distributions (see Figure 9b,d), however, a peak at about 130° in the vicinity of the solute

can be observed for TIP3P water, whereas such a feature is absent with the TIP4P model. Such a peak appears when the water molecule's oxygen is oriented exactly toward the solute cation, and the O-LP vectors form an angle of about 130° with $\vec{R}$. The dipole vector is then exactly collinear with the distance vector. This is consistent with ab initio calculations for strong charges like Mg^{2+} and Ca^{2+}.[36] However, the experiments by Soper et al.[37] show that the average angle of the dipoles for single charge ions, such as K^+, is between 40° and 50°. This corresponds to the situation in which one of the O-LP vectors points toward the cation, being rather antilinear with $\vec{R}$, another one protrudes outward at an angle of about 55−70°, and the 130° peak should not appear. On the basis of these indications, we conclude that the TIP3P model underestimates the influence of the surrounding water, most probably due to the smaller partial charges on hydrogens in this model compared to those in TIP4P. The differences between TIP3P and TIP4P results for cyclohexane (not shown) are not very drastic. However, TIP4P water seems again to give more plausible results for the distribution of dipoles orientations. The peaks in the 1HS are much better separated in TIP4P case, and their maxima are around 60° and 100°. These values are more reasonable than those found with TIP3P (70° and 105°) based on our theoretical analysis of the orientations. For large distances, the differences due to the different models are not so noticeable, but as our interest is focused mostly on the first hydration shell, the results for close distances are of much higher importance.

References and Notes

(1) Jalilihvand, F.; Spångberg, D.; Lindqvist-Reis, P.; Hermansson, K.; Persson, I.; Sandstroem, M. *J. Am. Chem. Soc.* **2001**, *123*, 431.
(2) McLain, S.; Imberti, S.; Soper, A. K.; Botti, A.; Bruni, F.; Ricci, M. A. *Phys. Rev. B* **2006**, *74*, 094201.
(3) Ikeda, T.; Boero, M.; Terakura, K. *J. Chem. Phys.* **2007**, *126*, 034501.
(4) Mueller, I. B.; Cederbaum, L. S.; Tarantelli, F. *J. Phys. Chem. A* **2004**, *108*, 5831.
(5) Asthagiri, D.; Pratt, L. R.; Paulaitis, M. E.; Rempe, S. B. *J. Am. Chem. Soc.* **2004**, *126*, 1285.
(6) Pauling, L.; Corey, R. B.; Branson, R. H. *Proc. Natl. Acad. Sci. U. S. A.* **1951**, *37*, 205.
(7) Pollack, G. H. *Cells, Gels, and the Engines of Life*; Ebner & Sons: Seattle, WA, U.S., 2001.
(8) Tanford, C. *Protein Sci.* **1997**, *6*, 1358.
(9) Ball, P. *Chem. Rev.* **2008**, *108*, 74.
(10) Dobson, C. M.; Sali, A.; Karplus, M. *Angew. Chem., Int. Ed. Engl.* **1998**, *37*, 868.
(11) Brooks, C. L.; Gruebele, M.; Onuchic, J. N.; Wolynes, P. G. *Proc. Natl. Acad. Sci. U. S. A.* **1998**, *95*, 11037.
(12) Tanford, C. *J. Mol. Biol.* **1972**, *67*, 59.
(13) Chandler, D. *Nature* **2005**, *437*, 640.
(14) Raschke, T.; Levitt, M. *Proc. Natl. Acad. Sci. U. S. A.* **2005**, *102*, 6777.
(15) Hille, B. *Ionic channels of excitable membranes*, 3rd ed.; Sinauer Associates Inc.: Sunderland, MA, U.S., 2001.
(16) MacKinnon, R.; Yellen, G. *Science* **1990**, *250*, 276.
(17) Lenaeus, M.; Vamvouka, M.; Focia, P. J.; Gross, A. *Nat. Struct. Mol. Biol* **2005**, *12*, 454.
(18) Guidoni, L.; Carloni, P. *J. Recept. Signal Trans.* **2002**, *22*, 315.
(19) Ahern, C. A.; Eastwood, A. L.; Lester, H. A.; Dougherty, D. A.; Horn, R. *J. Gen. Physiol.* **2006**, *128*, 649.
(20) Jorgensen, W.; Chandrasekhar, J.; Madura, J.; Impey, R.; Klein, M. *J. Chem. Phys.* **1983**, *79*, 926.
(21) Case, D. A. AMBER 9, 2006.
(22) Ryckaert, J. P.; Ciccotti, G.; Berendsen, H. J. C. *J. Comput. Phys.* **1977**, *23*, 327.
(23) Cornell, W. D.; Cieplak, P.; Bayly, C. I.; Gould, I. R.; Merz, K. M., Jr.; Ferguson, D. M.; Spellmeyer, D. C.; Fox, T.; Caldwell, J. W.; Kollman, P. A. *J. Am. Chem. Soc.* **1995**, *117*, 5179.
(24) Jakalian, A.; Bush, B.; Jack, D.; Bayly, C. *J. Comput. Chem.* **2000**, *21*, 132.
(25) Jakalian, A.; Jack, D.; Bayly, C. *J. Comput. Chem.* **2002**, *23*, 1623.
(26) Izaguirre, J. A.; Catarello, D. P.; Wozniak, J. M.; Skeel, R. D. *J. Chem. Phys.* **2001**, *114*, 2090.
(27) Berendsen, H. J. C.; Postma, J. P. M.; van Gunsteren, W. F.; DiNola, A.; Haak, J. R. *J. Chem. Phys.* **1984**, *81*, 3684.
(28) Dec, S.; Bowler, K.; Stadterman, L.; Koh, C.; E.D. Sloan, J. *J. Am. Chem. Soc.* **2006**, *128*, 414.
(29) Blokzijl, W.; Engberts, J. B. F. N. *Angew. Chem., Int. Ed. Engl.* **1993**, *32*, 1545.
(30) Southall, N.; Dill, K.; Haymet, A. *J. Phys. Chem. B* **2002**, *106*, 521.
(31) Cheng, Y.-K.; Rossky, P. *Nature* **1998**, *392*, 696.
(32) Yamakata, A.; Osawa, M. *J. Phys. Chem. Lett.* **2010**, *1*, 1487.
(33) Jorgensen, W. L.; Maxwell, D. S.; Tirado-Rives, J. *J. Am. Chem. Soc.* **1996**, *118*, 11225.
(34) Mobley, D.; Dumont, E.; Chodera, J.; Dill, K. *J. Phys. Chem. B* **2007**, *111*, 2242.
(35) Joung, I. S.; Cheatham, T. E., III. *J. Phys. Chem. B* **2008**, *112*, 9020.
(36) Krekeler, C.; Delle Site, L. *J. Phys.: Condens. Matter* **2007**, *19*, 192101.
(37) Soper, A.; Weckstroem, K. *Biophys. Chem.* **2006**, *124*, 180.

JP106282W